Microchimica Acta
https://doi.org/10.1007/s00604-018-3081-2

ORIGINAL PAPER

Dual-aptamer-based voltammetric biosensor for the *Mycobacterium tuberculosis* antigen MPT64 by using a gold electrode modified with a peroxidase loaded composite consisting of gold nanoparticles and a Zr(IV)/terephthalate metal-organic framework

Ningning Li[1] · Xing Huang[1] · Duanping Sun[1,2] · Weiye Yu[3] · Weiguo Tan[3] · Zhaofan Luo[4] · Zuanguang Chen[1]

Received: 21 August 2018 / Accepted: 31 October 2018

Abstract

An ultrasensitive aptasensor is described for the voltammetric determination of the *Mycobacterium tuberculosis* antigen MPT64 in human serum. Firstly, an amino-modified Zr(IV) based metal-organic framework (MOF; type UiO-66-NH_2; made up from Zr_6O_{32} units and 2-amino-terephthalate linkers) with a high specific surface was synthesized and used as the carrier of the gold nanoparticles and the aptamers. Then the signalling nanoprobe was fabricated after the horseradish peroxidase was cast on the nanomaterials. The two aptamers with synergistic effect on binding MPT64 were anchored on the gold electrode. Differential pulse voltammetry indicated that the peak current is highest if the ratio of the two aptamers is 1:1. The assay has a wide linear response range (0.02 to 1000 pg·mL^{-1} of MPT64) and a 10 fg·mL^{-1} detection limit at a working potential of around −96 mV (vs Ag/AgCl). The results show this biosensor to be a viable tool for detection of tuberculosis at an early stage.

Keywords Electrochemical aptasensor · *Mycobacterium tuberculosis* · MPT64 · UiO-66-NH_2 · Metal-organic framework · Horseradish peroxidase

Introduction

Tuberculosis (TB) is a lethal and common disease causing millions of deaths annually [1, 2]. The control of tuberculosis has already become a worldwide challenge for public health for the following reasons: the migration of people, the appearance of resistant strains of *Mycobacterium tuberculosis* and especially the HIV co-infection with MTB [3]. Therefore, rapid and accurate detection of MTB plays a major role in the early diagnosis and treatment of TB.

Numerous methods have been developed for the diagnosis of MTB, such as bacterial cultivation assay [4], specific nucleotide sequences diagnosis [5] and immunological detection [6]. The bacterial culture and smear microscopy methods are considered as the golden criterion and widely used in the detection of MTB. However, the disadvantages of the two method such as time consuming and low positive made them can hardly satisfy the demand of fast and accurate diagnosis [7]. Polymerase chain reaction (PCR) exhibits high sensitivity, reproducibility and specificity when applied it to the detection of specific nucleotide sequences of MTB. Nevertheless, complicated operation and strict demand for the experimental conditions which are hard to afford for most primary medical units [8].

Electronic supplementary material The online version of this article (https://doi.org/10.1007/s00604-018-3081-2) contains supplementary material, which is available to authorized users.

✉ Duanping Sun
sundp@gdpu.edu.cn

✉ Zuanguang Chen
chenzg@mail.sysu.edu.cn

[1] School of Pharmaceutical Sciences, Sun Yat-Sen University, Guangzhou 510006, China

[2] Center for Drug Research and Development, Guangdong Pharmaceutical University, Guangzhou 510006, China

[3] Shenzhen Center for Chronic Disease Control, Shenzhen 518020, China

[4] The Seventh Affiliated Hospital of Sun Yat-Sen University, Shenzhen 518071, China

Published online: 12 November 2018

According to the early research [9, 10], MPT64 is a kind of 24-kDa protein only secreted by MTB in the early and middle period of bacterial growth. This protein can be utilized for the specific early detection of MTB [11, 12]. And thanks to Qin's efforts, the aptamers which can specifically bind to MPT64 had already been discovered [13]. Aptamers are oligonucleic acid or peptide molecules. It has considerable advantages such as conveniently screen, reproducibly synthesis, easy to label, immobilize, signal and regenerate, most importantly, adaptability to various targets (small molecules [14], proteins [15], and cells [16]). Electrochemical aptasensor as a robust analytical tools has aroused tremendous attention for its high sensitivity, selectivity, and reproducibility to the early diagnosis of various diseases [17]. Though the electric methods have many merits, the sensitivity is still not high enough to satisfy the demand of clinical sample analysis [16]. For purpose of boosting the electrochemical aptasensor detection sensitivity, amount of electro catalysts or nanoprobes have been designed to amplify the detection signal. Loading enzymes on nanoparticles is a common method to enhance the signal, such as cast horseradish peroxidase onto nanomaterials [18]. Therefore, it has great significance to explore some new nanomaterials to increase the detection sensitivity.

Taking advantage of nanotechnology, an increasing number of nanomaterials were successfully synthesized and employed in the field of electrochemical detection. Metal-organic frameworks (MOFs), a new class of hybrid and porous material, have aroused the tremendous attention of people. MOFs consist of organic linkers and metal ions and are connected by a coordinate bond to form reticular crystalline structure [19]. The increasing number of applications in the last few years indicated the great potential of these new materials [20, 21]. Due to the outstanding physical and chemical properties of MOFs concluding high surface area, adjustable chemical composition and surface functionality, and well-defined metal sites [22], they are widely regarded as promising candidates for the fixing of many substances, for instance, metal nanoparticles and enzymes [23, 24]. UiO-66-NH_2, a zirconium containing MOF, has a crystalline structure made up by hexameric Zr_6O_{32} units and 2-amino-terephthalate linkers [25]. Moreover, UiO-66-NH_2 has amino groups which make it easier to link metal ions on the materials [26].

We chose UiO-66-NH_2 as the enzyme nanocarrier for that it has high stability, regular shape, ultra-high surface area and amino groups on its surface [27]. The surface of MOF was anchored with gold nanoparticles (AuNPs) by a one-step hydrothermal synthesis method. To our knowledge, there have not been any targeted investigation on detecting MTB by using the AuNPs/UiO-66-NH_2. According to earlier research, two aptamers are utilized for capturing MPT64. There are some reports that researchers anchored two different aptamers on electrode to detect different proteins [28, 29] or cells [30, 31], respectively. For the first time, we incubated gold electrode with the mixture aptamers to enhance the detection sensitivity. We found that it had higher signal compared with using single aptamer to capture MPT64. The aptasensor had good performance on detecting MPT64 with a low detection limit at 10 fg·mL^{-1} and had great potential in the early detection of TB.

Experimental

Materials and reagents

Zirconium chloride ($ZrCl_4$), 2-aminoterephthalic acid (NH_2-H_2BDC) were purchased from Macklin Biochemical Co., Ltd. (Shanghai, China, http://www.macklin.cn/). MPT64 protein was obtained from Detai Biologics Co., Ltd. (Nanjing, China, http://www.detaibio.com/) and CFP10-ESAT6 was purchased from Beijing Protein Innovation. Co. Ltd. (Beijing, China http://www.proteomics.org.cn/). BSA (bovine serum albumin) was purchased from Sigma-Aldrich Chem. Co. (St. Louis, MO, USA, http://www.sigmaaldrich.com/chinamainland.html). Tris (2-carboxyethyl)phosphine hydrochloride (TCEP) (a buffer containing 10 mM Tris–HCl buffer and 1 mM TCEP, pH 7.4) was purchased from Sangon Biotech. Co. Ltd. (Shanghai China, http://www.sangon.com/), horseradish peroxidase (HRP), dimethylformamide (DMF), H_2O_2 (30%, *w*/w), 6-Mercapto-1-hexanol (MCH), hydroquinone (HQ), poly (vinyl pyrrolidone) (PVP, MW 40 k) and chloroauric acid ($HAuCl_4{\cdot}4H_2O$) were obtained from Aladin Chemistry Co., Ltd. (Shanghai, China, http://www.aladdin-e.com/). The synthesis and purification of thiolated aptamers were accomplished by Sangon Biotech Co., Ltd. (Shanghai China, http://www.sangon.com/). The sequence are as follows and the secondary structure of APT-I and APT-II were showed in Fig. S1):

APT-I: 5'-SH-$(CH_2)_6$-TGGGAGCTGATGTCGCATGG GTTTTGATCACATGA-3'
APT-II: 5'-SH-$(CH_2)_6$-TTCGGGAATGATTATCAAAT TTATGCCCTCTGAT-3′

Phosphate buffered saline (PBS) (pH 7.0, 100 mM) employed as a working solution and PBS of pH 9.0 used to the preparation of signal nanoprobe were prepared with $Na_2HPO_4{\cdot}12H_2O$ (62 mM), KH_2PO_4 (38 mM), NaCl (137 mM) and KCl (2.7 mM). Ultrapure water (18.2 MΩ·cm resistivity, Milli-Q, Millipore) was used for all the experiments. All reagents were of analytical grade and were used without further purification.

Apparatus

The field emission scanning electron micrographs (SEM; Geminni500, Germany, https://www.fei.com/home/), Transmission electron microscopy (TEM; FEI Tecnai G2 Spirit, Netherlands, https://www.fei.com/home/) and X-ray photoelectron spectroscopy (XPS, ESCALAB 250Xi, Thermo Scientific, USA, https://www.thermofisher.com/cn) were applied to characterize the morphologies and structures of the samples we synthesized.

Electrochemical measurements

All electrochemical measurements were accomplished by using a CHI660E electrochemical workstation (Shanghai Chenhua Instrument Co., Ltd. Shanghai, China, http://www.chinstr.com/). A conventional three-electrode system containing a platinum wire counter electrode, an Ag/AgCl reference electrode (the KCl concentration in the reference electrode is saturated solution) and a bare gold electrode (3 mm in diameter) as the working electrode (Gaoss Union Technology Co., Ltd. Wuhan, China, http://gaossunion.cn.china.cn/) was applied. The electrode fabrication was characterized by electrochemical impedance spectroscopy (EIS) which were performed in 5 mM $[Fe(CN)_6]^{4-/3-}$ solution containing 0.5 M KCl (frequency range of 0.01 Hz to 100 kHz and an amplitude of a 10 mV). Differential pulse voltammetry (DPV) measurements were performed in 0.1 M PBS (a saline buffer containing 3 mM H_2O_2 and 2 mM HQ) to investigate the performance of the biosensor. The working parameters were: 50 ms pulse width, 50 mV pulse amplitude, 0.1 s pulse period and voltage from 0.1 to −0.3 V.

Preparation of AuNP/UiO-66-NH_2 nanoparticles

AuNPs/UiO-66-NH_2 nanoparticles were prepared according to the previous article with minor adjustments [27]. Briefly, 0.12 g of $ZrCl_4$, 0.093 g of NH_2·H_2BDC and 0.60 g PVP were dissolved in 30 mL DMF-ethanol (*v*/v = 4:1) mixed solution in a 50 mL Teflon liner. After dissolved thoroughly, 60 μL of 1 g·mL^{-1} $HAuCl_4$·$4H_2O$ solution was added into Teflon liner, and then allowed to react at 120 °C for 24 h without stirring. The samples were collected, washed with fresh DMF and ultrapure water for three times, relatively.

Preparation of the aptamer/HRP/AuNP/UiO-66-NH_2 nanoprobes

Firstly, the previous synthetic nanoparticles were suspended in PBS (saline of pH 9.0; 100 mM, 1 mg·mL^{-1}). Then 10 μL of the aptamers (APT-I:APT-II = 1:1, V: V, 5 mM) which was already incubated with 1 mM TCEP for 1 h at room temperature was added into the solution. Then gently stirring the resulting solution for 24 h at 4 °C. Finally added 50 μL of HRP (1 mg·mL^{-1}) to the above solution, then the resulting mixture was incubated at 4 °C for another 1 h under gentle stirring to form Aptamer/HRP/AuNPs/UiO-66-NH_2 nanoprobes. The already synthesized Aptamer/HRP/AuNPs/UiO-66-NH_2 nanoprobes were collected and washed with fresh saline buffer solution.

Construction of the aptasensor

Scheme 1 shows the fabrication process of the nanoprobe and the detecting mechanism of the aptasensor. Prior to use, the

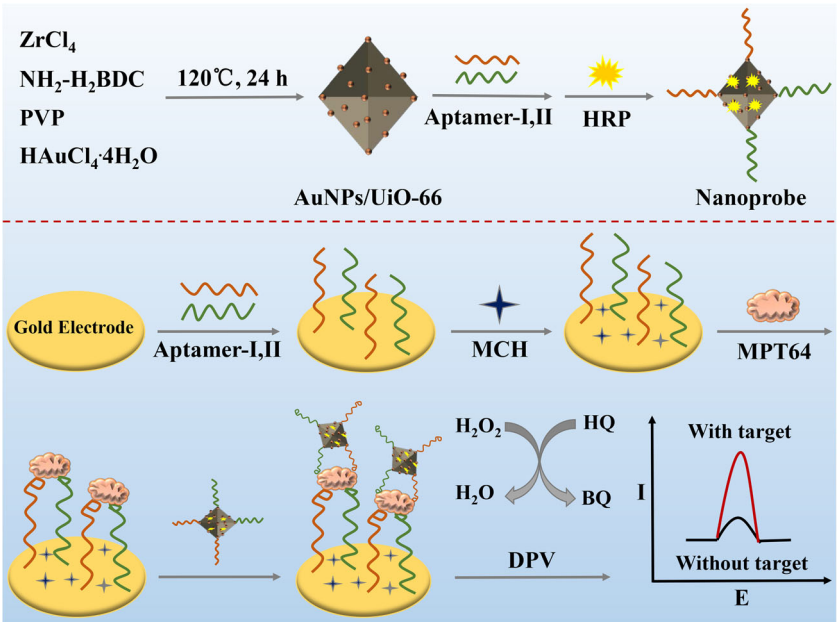

Scheme 1 The process of the fabrication of the aptamer/HRP/AuNPs/UiO-66-NH_2 nanoprobes and the electrochemical aptasensor. (PVP: poly (vinyl pyrrolidone); HRP: horseradish peroxidase; MCH: 6-Mercapto-1-hexanol; HQ: hydroquinone; BQ: benzoquinone)

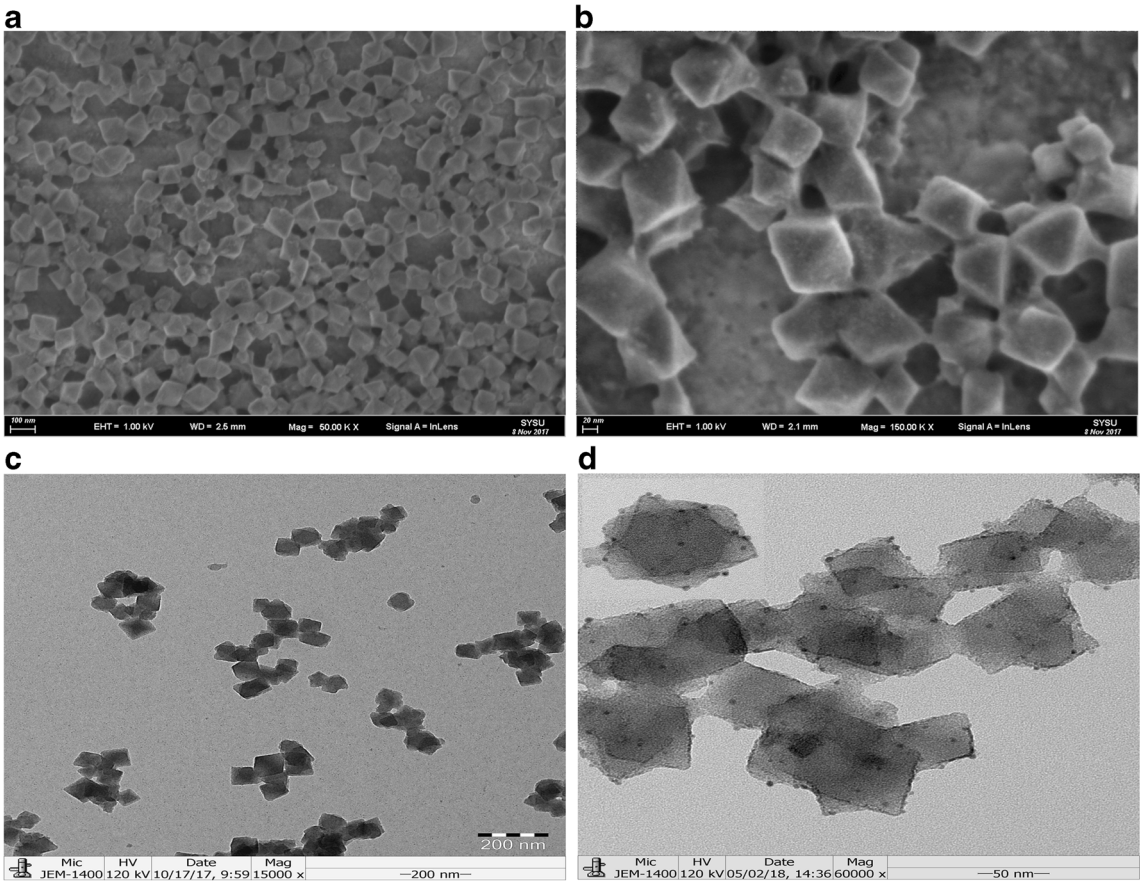

Fig. 1 The SEM (**a**, **b**) and TEM (**c**, **d**) images of AuNPs/UiO-66-NH_2.The scale bar were 100 nm (**a**), 20 nm (**b**), 200 nm (**c**) and 50 nm (**d**)

gold electrodes were soaked with piranha solution (98% H_2SO_4/ 30% H_2O_2 = 3:1, *v*/v) for 15 min. Then, 0.3 μM and 0.05 μM alumina slurry were used to polish the electrodes and ultrasonic sequentially in ultrapure water, ethanol and ultrapure water for about 3 min, relatively. Then the electrodes were further electrochemically cleaned in 0.5 M H_2SO_4 and the potential scanning was from −0.2 to 1.5 V. Firstly, reduce the disulfide bonds of the thiolated aptamers (APT-I: APT-II = 1:1, V: V) (0.5 μM) with 1 mM TCEP for 1 h at room temperature in darkness. Subsequently, immersed the already prepared gold electrode to the mixture solution mentioned above at room temperature in humidity for 12 h and washed with ultrapure water to remove the redundant aptamers. After that, 1 mM MCH solution was used to block the uncovered active site of the gold electrode. After that, the electrode was incubated in 70 μL PBS solution concluding the target MPT64 protein at different concentrations for 90 min at 37 °C. Finally, a droplet of 10 μL signal nanoprobe was dropped onto the modified electrode for another 90 min. The DPV measurements was used for the analysis of

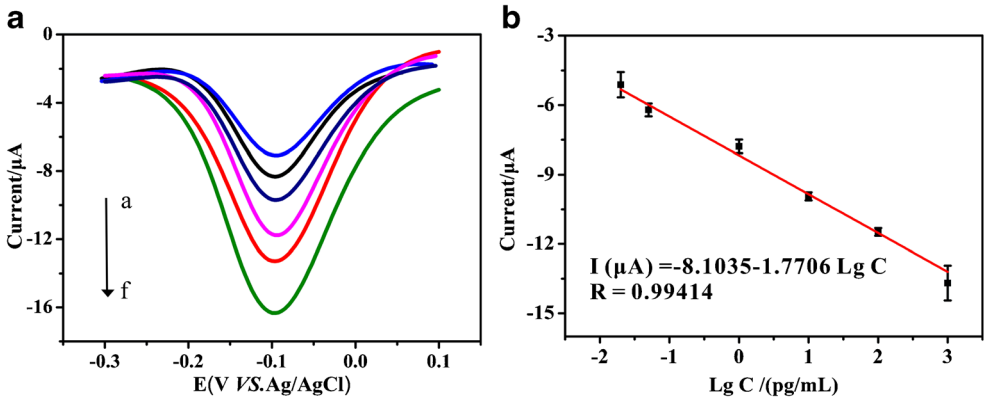

Fig. 2 DPV responses of the aptasensor after incubation with different concentrations (a to f, 0.02, 0.05, 1, 10, 100, 1000 pg·mL^{-1}) of MPT64 in 0.1 M PBS (saline of pH 7.0) containing 3 mM HQ and 2 mM H_2O_2. Working parameters of DPV: 50 ms pulse width, 50 mV pulse amplitude, 0.1 s pulse period and scan from 0.1 to −0.3 V

Table 1 Comparison of different methods for MTB detection

Detection method	Target	Linear range	Detection limit	Ref.
Impedance	Heat shock protein	100 fM −1 nM	100 fM	[32]
ELISA	MPT64	2.1–250 ng·mL^{-1}	2.1 ng·mL^{-1}	[6]
Voltammetry	MPT64	0.02–1000 pg·mL^{-1}	20 fg·mL^{-1}	[33]
Voltammetry	MPT64	0.02–1000 pg·mL^{-1}	10 fg·mL^{-1}	This work

Mycobacterium tuberculosis antigen MPT64. The parameters of DPV measurements were from 0.1 to −0.3 V with a 50 mV pulse amplitude in degassed 100 mM PBS (pH 7.0) including 2 mM H_2O_2 and 3 mM HQ.

Results and discussion

Characterization of the nanomaterials

The morphology and structure of AuNPs/UiO-66-NH_2 nanocomposites were investigated by different characterization techniques. The SEM images of AuNPs/UiO-66-NH_2 shows that the crystal structures exhibited octahedral geometry (Fig. 1a and b), which indicated that the crystal structure of UiO-66-NH_2 did not affected by the AuNPs. As Fig. 1b shows, plenty of Au particles were attached to the surface of MOF, indicating that the AuNPs/UiO-66-NH_2 were successfully prepared. The TEM images of AuNPs/UiO-66-NH_2 (Fig. 1c and d) exhibits intact crystal morphology with average dimension about 100 nm. The XPS result of AuNPs/UiO-66-NH_2 is listed in Fig. S2 and S3.

Electrochemical characterization of the biosensor

EIS results were applied to confirm the stepwise modification process of the electrode. The results and detailed discussion of EIS is shown in the Electronic Supplementary Material (Fig. S4).

Optimization of method

The following parameters were optimized: (a) Different ratio of the capture probe (Fig. S5) and (b) HQ concentration (Fig. S6). Respective data and Figures are given in the Electronic Supporting Material. The following experimental conditions were found to give best results: (a) Best ratio of the capture probe: 1:1 (APT-I: APT-II); (b) Optimal HQ concentration: 3 mM. Therefore, 3 mM HQ and 2 mM H_2O_2 was regarded as the optimal concentration for the subsequent experiments.

Performances of the aptasensor in MPT64 detection

Sensitivity plays a crucial role in the evaluation of the electrochemical aptasensor. DPV response of the sensing method to different concentrations of MPT64 was performed under optimized experimental conditions. The current change of DPV is described in Fig. 2a, it shows that with the increase of the account of standard MPT64 solution from 0.02 to 1000 pg·mL^{-1}, the peak current of the platform gradually increased, respectively. The calibration plot related to different concentrations of MPT64 is depicted in Fig. 2b. It indicated that the DPV responses was proportional to the logarithm value of MPT64 and the R value was 0.99664. The regression equation is I (μA) = −8.1543-1.7625 Lg C (pg·mL^{-1}) and the estimated detection limit is as low as 10 fg·mL^{-1}. The detection limit was obtained according to the 3σ method. The comparison results of this aptasensor we constructed with other reported

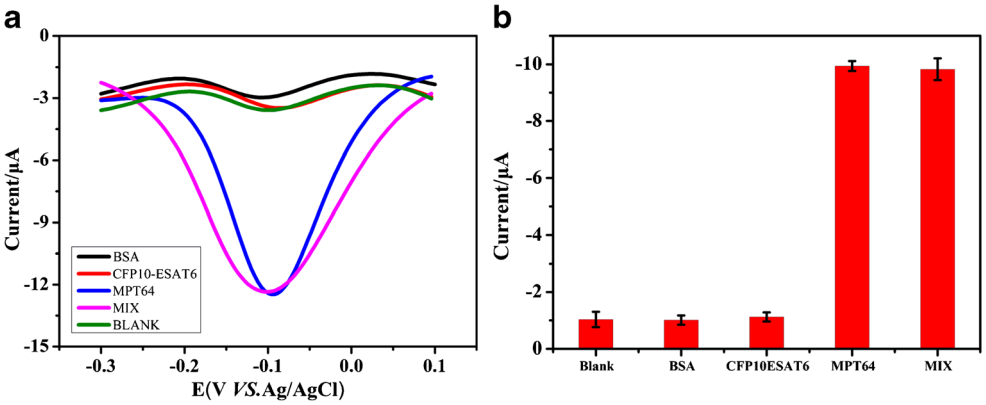

Fig. 3 DPV responses (**a**) and the corresponding histogram (**b**) of the resulting aptasensor toward different analytes. The error bars represent the standard deviations of three parallel determination results. (Working parameters of DPV: 50 ms pulse width, 50 mV pulse amplitude, 0.1 s pulse period and voltage from 0.1 to −0.3 V)

detection methods for *MTB* detection is listed in Table 1. Through the comparison, the biosensor has a wider linear range and a lower detection limit. The reason maybe account for the dual-aptamer system and the ultra-high surface of the nanomaterial which anchored more AuNPs and HRP.

Specificity and reproducibility of the biosensor

It is a very complex environment of the serum and there are some substances may affect the detection results. In this research, bovine serum albumin (BSA), CFP-10-EAST-6 antigen complex (CFP10-ESAT6), the mixture of MPT64 and CFP10-ESAT6, were employed to investigate the selectivity of the aptasensor. Fig. 3a and b show that the DPV responses of these nonspecific interferents (BSA, CFP10-ESAT-6, 1 ng·mL^{-1}) is not different if compared with the DPV response of the blank. When the aptasensor was prepared to detect target protein, MPT64, the current had a significant rise even the concentration was 100 fold lower (10 pg·mL^{-1}) over the interfering agents and it had severe difference between the target MPT64 and the mixture protein. The DPV results showed the aptasensor we fabricated had satisfactory selectivity.

To evaluate the reproducibility of the aptasensor, five electrodes, operated in the same way, were used to detect the same concentration of target protein (10 pg·mL^{-1}). The DPV responses of each electrode had subtle difference with a relative standard deviation (RSD) of 5.2%, indicting a good reproducibility of the sensor.

Performance of the assay in human serum

The standard addition method was chose to assess the electrochemical aptasensor in serum by adding the target protein into the health human serum and the results are displayed in Electronic supplementary material Table S1. The recovery rate for the MPT64 added to the diluted health human serum range from 95.9% to 111.6%. The results demonstrated that the electrochemical aptasensor can be potentially applied in real sample and used to the quantitative detection of MPT64.

Conclusion

We describe an electrochemical aptasensor for the ultrasensitive detection of MPT64 based on the dual-aptamer (APT-I and APT-II) and the hybrid signal-amplifying nanoprobes. The MOF has a large surface area. Therefore, more AuNPs and HRP can be immobilized. This has a beneficial effect on the amplification of signal and the sensitivity of the detection. And we mixed the two aptamers of MPT64 and immobilized it on the gold electrode to bind to the target protein. The results of DPV responses demonstrated that this approach did promote the detection sensitivity. The aptasensor had eminent performance in the detection of MPT64 with wide linear range, great selectivity and a low detection limit. The biosensor do exist some defects such as it still has some difficulty on clinical application and the modification process of electrode will be affected by various factors. In the future, the combination of electrochemical detection and other device such as microfluidic chip may solve those flaws mentioned above and well used in the clinical detection.

Acknowledgements This work was supported by the National Natural Science Foundation of China (No. 21675177), the Science and Technology Planning Project of Guangdong Province (No. 2016B030303002), the Natural Science Foundation of Guangdong Province (No. 2018A030310142), and the Medical Scientific Research Foundation of Guangdong Province (No. A2017033).

Compliance with ethical standards The author(s) declare that they have no competing interests.

References

1. Farid S, Meshik X, Choi M, Mukherjee S, Lan Y, Parikh D, Poduri S, Baterdene U, Huang CE, Wang YY, Burke P, Dutta M, Stroscio MA (2015) Detection of interferon gamma using graphene and aptamer based FET-like electrochemical biosensor. Biosens Bioelectron 71:294–299
2. Zumla A, George A, Sharma V, Herbert RHN, Masham of Ilton B, Oxley A, Oliver M (2015) The WHO 2014 global tuberculosis report-further to go. Lancet Glob Health 3:E10–E12
3. Mi XW, He FJ, Xiang MY, Lian Y, Yi SL (2012) Novel phage amplified multichannel series piezoelectric quartz crystal sensor for rapid and sensitive detection of Mycobacterium tuberculosis. Anal Chem 84:939–946
4. Mejia GI, Castrillon L, Trujillo H, Robledo JA (1999) Microcolony detection in 7H11 thin layer culture is an alternative for rapid diagnosis of Mycobacterium tuberculosis infection. Int J Tuberc Lung D 3:138–142
5. Moure R, Munoz L, Torres M, Santin M, Martin R, Alcaide F (2011) Rapid detection of Mycobacterium tuberculosis complex and rifampin resistance in smear-negative clinical samples by use of an integrated real-time PCR method. J Clin Microbiol 49:1137–1139
6. Ji M, Cho B, Cho YS, Park SY, Cho SN, Jeon BY, Yoon BS (2014) Development of a quantitative sandwich enzyme-linked immunosorbent assay for detecting the MPT64 antigen of Mycobacterium tuberculosis. Yonsei Med J 55(3):746–752
7. Mehaffy C, Dobos KM, Nahid P, Kruh-Garcia NA (2017) Second generation multiple reaction monitoring assays for enhanced detection of ultra-low abundance Mycobacterium tuberculosis peptides in human serum. Clin Proteomics 14:21
8. Theron G, Peter J, van Zyl-Smit R, Mishra H, Streicher E, Murray S, Dawson R, Whitelaw A, Hoelscher M, Sharma S, Pai M, Warren R, Dheda K (2011) Evaluation of the Xpert MTB/RIF assay for the diagnosis of pulmonary tuberculosis in a high HIV prevalence setting. Am J Respir Crit Care Med 184:132–140
9. Jiang Y, Liu HC, Wan KL (2014) MPT64 polymorphisms of Mycobacterium tuberculosis strains suggest ongoing immune evasion. Tuberculosis 94:712–714
10. Yin XM, Zheng L, Lin L, Hu YR, Zheng F, Hu YW, Wang Q (2013) Commercial MPT64-based tests for rapid identification of Mycobacterium tuberculosis complex: a meta-analysis. J Inf Secur 67:369–377

11. Thakur H, Kaur N, Sabherwal P, Sareen D, Prabhakar N (2017) Aptamer based voltammetric biosensor for the detection of Mycobacterium tuberculosis antigen MPT64. Microchim Acta 184(7):1915–1922
12. Gou D, Xie G, Li Y, Zhang X, Chen H (2018) Voltammetric immunoassay for Mycobacterium tuberculosis secretory protein MPT64 based on a synergistic amplification strategy using rolling circle amplification and a gold electrode modified with graphene oxide, Fe_3O_4 and Pt nanoparticles. Microchim Acta 185(9):1–9
13. Qin LH, Zheng RJ, Ma ZX, Feng YH, Liu ZH, Yang H, Wang J, Jin RL, Lu JM, Ding YS, Hu ZY (2009) The selection and application of ssDNA aptamers against MPT64 protein in Mycobacterium tuberculosis. Clin Chem Lab Med 47:405–411
14. Zhou M, Zhai YM, Dong SJ (2009) Electrochemical sensing and biosensing platform based on chemically reduced graphene oxide. Anal Chem 81:5603–5613
15. Yang J, Dou B, Yuan R, Xiang Y (2016) Proximity binding and metal ion-dependent DNAzyme cyclic amplification-integrated aptasensor for label-free and sensitive electrochemical detection of thrombin. Anal Chem 88:8218–8223
16. Sun DP, Lu J, Zhong YW, Yu YY, Wang Y, Zhang BB, Chen ZG (2016) Sensitive electrochemical aptamer cytosensor for highly specific detection of cancer cells based on the hybrid nanoelectrocatalysts and enzyme for signal amplification. Biosens Bioelectron 75:301–307
17. Zheng TT, Tan TT, Zhang QF, Fu JJ, Wu JJ, Zhang K, Zhu JJ, Wang H (2013) Multiplex acute leukemia cytosensing using multifunctional hybrid electrochemical nanoprobes at a hierarchically nanoarchitectured electrode interface. Nanoscale 5:10360–10368
18. Zheng TT, Zhang QF, Feng S, Zhu JJ, Wang Q, Wang H (2014) Robust nonenzymatic hybrid nanoelectrocatalysts for signal amplification toward ultrasensitive electrochemical cytosensing. J Am Chem Soc 136:2288–2291
19. Zhou HC, Long JR, Yaghi OM (2012) Introduction to metal-organic frameworks. Chem Rev 112:673–674
20. Gascon V, Castro-Miguel E, Diaz-Garcia M, Blanco RM, Sanchez-Sanchez M (2017) In situ and post-synthesis immobilization of enzymes on nanocrystalline MOF platforms to yield active biocatalysts. J Chem Technol Biotechnol 92:2583–2593
21. Ricco R, Pfeiffer C, Sumida K, Sumby CJ, Falcaro P, Furukawa S, Champness NR, Doonan CJ (2016) Emerging applications of metal-organic frameworks. Crystengcomm 18:6532–6542
22. Sabyrov K, Jiang J, Yaghi OM, Somorjai GA (2017) Hydroisonnerization of n-hexane using acidified metal-organic framework and platinum nanoparticles. J Am Chem Soc 139: 12382–12385
23. Feng DW, Liu TF, Su J, Bosch M, Wei ZW, Wan W, Yuan DQ, Chen YP, Wang X, Wang KC, Lian XZ, Gu ZY, Park J, Zou XD, Zhou HC (2015) Stable metal-organic frameworks containing single-molecule traps for enzyme encapsulation. Nat Commun 6:5979
24. Li L, Yuan Y, Chen Y, Zhang P, Bai Y, Bai L (2018) Aptamer based voltammetric biosensor for Mycobacterium tuberculosis antigen ESAT-6 using a nanohybrid material composed of reduced graphene oxide and a metal-organic framework. Microchim Acta 185(8):379
25. Shen LJ, Wu WM, Liang RW, Lin R, Wu L (2013) Highly dispersed palladium nanoparticles anchored on UiO-66(NH_2) metal-organic framework as a reusable and dual functional visible-light-driven photocatalyst. Nanoscale 5:9374–9382
26. Guo ZY, Xiao CX, Maligal-Ganesh RV, Zhou L, Goh TW, Li XL, Tesfagaber D, Thiel A, Huang WY (2014) Pt nanoclusters confined within metal organic framework cavities for chemoselective cinnamaldehyde hydrogenation. ACS Catal 4:1340–1348
27. Ling PH, Lei JP, Jia L, Ju HX (2016) Platinum nanoparticles encapsulated metal-organic frameworks for the electrochemical detection of telomerase activity. Chem Commun 52:1226–1229
28. Szymanski M, Noble J, Knight A, Porter R, Worsley G (2013) Aptamer-mediated detection of thrombin using silver nanoparticle signal enhancement. Anal Methods 5:187–191
29. Li XM, Liu JM, Zhang SS (2010) Electrochemical analysis of two analytes based on a dual-functional aptamer DNA sequence. Chem Commun 46:595–597
30. Min K, Song KM, Cho M, Chun YS, Shim YB, Ku JK, Ban C (2010) Simultaneous electrochemical detection of both PSMA (+) and PSMA (−) prostate cancer cells using an RNA/peptide dual-aptamer probe. Chem Commun 46:5566–5568
31. Qu LM, Xu JH, Tan XF, Liu Z, Xu LG, Peng R (2014) Dual-aptamer modification generates a unique interface for highly sensitive and specific electrochemical detection of tumor cells. ACS Appl Mater Interfaces 6:7309–7315
32. Gopinath SCB, Perumal V, Kumaresan R, Lakshmipriya T, Rajintraprasad H, Rao BS, Arshad MKM, Chen Y, Kotani N, Hashim U (2016) Nanogapped impedimetric immunosensor for the detection of 16 kDa heat shock protein against Mycobacterium tuberculosis. Microchim Acta 183(10):2697–2703
33. Bai L, Chen Y, Bai Y, Chen Y, Zhou J, Huang A (2017) Fullerenedoped polyaniline as new redox nanoprobe and catalyst in electrochemical aptasensor for ultrasensitive detection of Mycobacterium tuberculosis MPT64 antigen in human serum. Biomaterials 133:11–19